

Signatures of Dynamical Tunneling in the Wave function of a Soft-Walled Open Microwave Billiard

Y.-H. Kim,¹ U. Kuhl,¹ H.-J. Stöckmann,¹ and J. P. Bird²

¹*Fachbereich Physik der Philipps-Universität Marburg, Renthof 5, D-35032 Marburg, Germany*

²*Department of Electrical Engineering, the University at Buffalo, Buffalo, NY 14260-1920, USA*

(Dated: November 19, 2018)

Evidence for dynamical tunneling is observed in studies of the transmission, and wave functions, of a soft-walled microwave cavity resonator. In contrast to previous work, we identify the conditions for dynamical tunneling by monitoring the evolution of the wave function phase as a function of energy, which allows us to detect the tunneling process even under conditions where its expected level splitting remains irresolvable.

PACS numbers: 73.23.-b, 73.23.Ad, 85.35.Be, 72.20.-i

The term dynamical tunneling has been used to refer to the phenomenon in which quantum-mechanical particles, confined within some system, are able to access regions of phase space, inaccessible to their classical counterparts [1, 2, 3]. This process is distinct from tunneling in the usual sense, since the "tunnel barrier" is provided by the existence of classically-forbidden regions of phase space, rather than the presence of any potential barrier. Recently, there has been much interest in the manifestations of dynamical tunneling in a number of different physical systems, such as cold atoms localized in a superlattice potential [4, 5], superconducting microwave cavities [6], and open quantum dots realized in the high-mobility two-dimensional electron gas of semiconductor heterojunctions [7, 8, 9]. Effort in these studies has focused on demonstrating the measurable signatures of dynamical tunneling, such as time-resolved oscillations of cold atoms due to tunneling between symmetric KAM-island structures [4, 5], tunnel splitting in the eigenspectrum of microwave cavities [6], and periodic conductance oscillations in quantum dots [7, 8, 9]. The details of the tunneling are expected to be strongly influenced by the structure of the classical phase space, and in Ref. [4] it was found that the tunneling rate could be strongly influenced by the presence of chaos in the corresponding classical dynamics (chaos-assisted tunneling).

Recently, we have explored the use of open microwave cavities, as an analog system for the investigation of transport in quantum-dot nanostructures. Such investigations are made possible by the equivalence, for a two-dimensional system, of the Schrödinger and Helmholtz equations, according to which a measurement of the electric field within the cavity is analogous to the wave function in the corresponding quantum dot [10]. Our previous work in this area has focused on investigations of the phenomena exhibited by hard-walled cavities, which we have used to detect evidence for wave function scarring [11], and to investigate the influence of a single impurity of the wave function in quantum dots [12]. In this Letter, however, we report on the use of a novel technique to identify the existence of dynamical tunneling, in studies of a soft-walled microwave resonator. To the best of our

knowledge, there has previously only been one report on the implementation of a soft-walled microwave resonator, in the unpublished thesis of Lauber [12]. Such soft-walled cavities are of particular interest, since they mimic the form of the potential profile that is found in studies of typical quantum dots [13]. The soft walls give rise to a mixed phase space, with well-defined KAM islands that are separated by classically impenetrable regions [9, 14]. In previous studies of quantum dots, an analysis of the oscillations in their magneto-conductance was argued to provide a signature of dynamical tunneling of electrons, onto such an island [9]. In this Letter, we demonstrate a novel manifestation of dynamical tunneling in a soft-walled microwave resonator, by studying the evolution of the phase of the wave function in the cavity, as a function of energy (i.e. frequency). In terms of the notation introduced by Heller [15], our study reveals the existence of "dirty" states in the wave function, which are generated from a pair of "clean" states, degenerate in energy, are degraded by their tunneling interaction.

In a microwave resonator with parallel top and bottom plates, the electric field, $E(x, y, z)$, points from top to bottom plates, the electric field $E(x, y, z)$ points from top to bottom in the z direction for the lowest modes, the transverse magnetic modes. In the three-dimensional Helmholtz equation for $E(x, y, z)$, the z dependence can be separated out, resulting in a two-dimensional Helmholtz equation for $E(x, y)$

$$\left[-\Delta_{xy} + \left(\frac{n\pi}{d}\right)^2\right] E(x, y) = k^2 E(x, y), \quad (1)$$

where k is the wave number, d the height of the resonator, and n the k_z quantum number. For $n = 0$ this is equivalent to the stationary Schrödinger equation for a two-dimensional billiard with Dirichlet boundary condition, which has been used in numerous experiments [10]. For $n = 1$, however, the additional term can be used to mimic a potential $V(x, y)$ by putting

$$d(x, y) \sim \frac{1}{\sqrt{V(x, y)}}. \quad (2)$$

The approach is not exact, since the separation of the

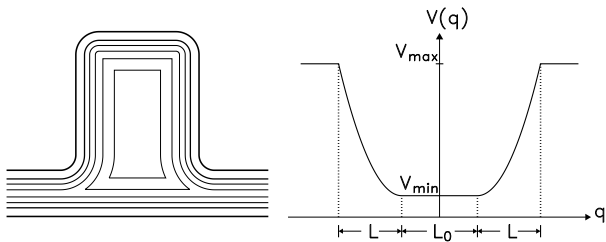


FIG. 1: (a) Height profile of the resonator. The top is 10.4 mm above the bottom, between neighboring contour lines, there is a height difference of 2.08 mm, (b) corresponding potential $V(q)$ along a cut, where $L = 50$ mm, and $L_0 = 60$ mm, 140 mm, 152 mm for the vertical, horizontal, and diagonal cut, respectively.

z component works for constant d only, but as long as the potential variation is small on the scale of the wave length, the error terms can be neglected.

Fig. 1(a) shows a sketch of the resonator used together with its height profile. The minimum distance between the top and bottom plate was $d_{\min} = 6.3$ mm outside the resonator increasing gradually to $d_{\max} = 16.7$ mm in the bottom of the resonator. Due to a small and unavoidable misalignment of the top plate there were variations of the height over the area of the resonator of up to 0.9 mm. The corresponding potential was constant in the bottom of the dot and increased quadratically close to the boundaries, both in the vertical and perpendicular direction as well as along the diagonals, see Fig. 1(b). Such potential shapes are typical for quantum dots realized by remote surface gates [13].

Two antennas A_1 and A_2 serving as source and drain for the microwaves, were attached to the leads, which were closed by absorbers. A third antenna A_3 was moved on a quadratic grid of period 5 mm to map out the field distribution within the dot. Details can be found in our previous publications [11, 16]. For $\nu_{\min} = c/(2d_{\max}) = 9$ GHz only the $n = 0$ modes exist. They are not observed, however, since the billiard is open in the xy plane. For $\nu_{\min} < \nu < \nu_{\max} = c/d_{\max} = 18$ GHz the $n = 1$ modes exist as well. Another frequency threshold of relevance is found at $\nu_T = 12.5$ GHz. Below this frequency all $n = 1$ states are bound whereas for higher frequencies the states extend into the attached channels and have thus to be interpreted as resonance states.

Fig. 2 shows the modulus of the transmission S_{21} between antenna A_1 in the entrance and antenna A_2 in the exit wave guide, together with the modulus of the reflection S_{33} at the movable antenna A_3 at a fixed position within the billiard in the upper panel. The solid vertical line at 12.5 GHz corresponds to the threshold frequency ν_T where the billiard states can couple to the wave guides. Correspondingly, the transmission is close to 0 below this frequency. The vertical dotted lines correspond to a number of selected resonance eigenfrequencies, the corresponding wave functions for which are shown in

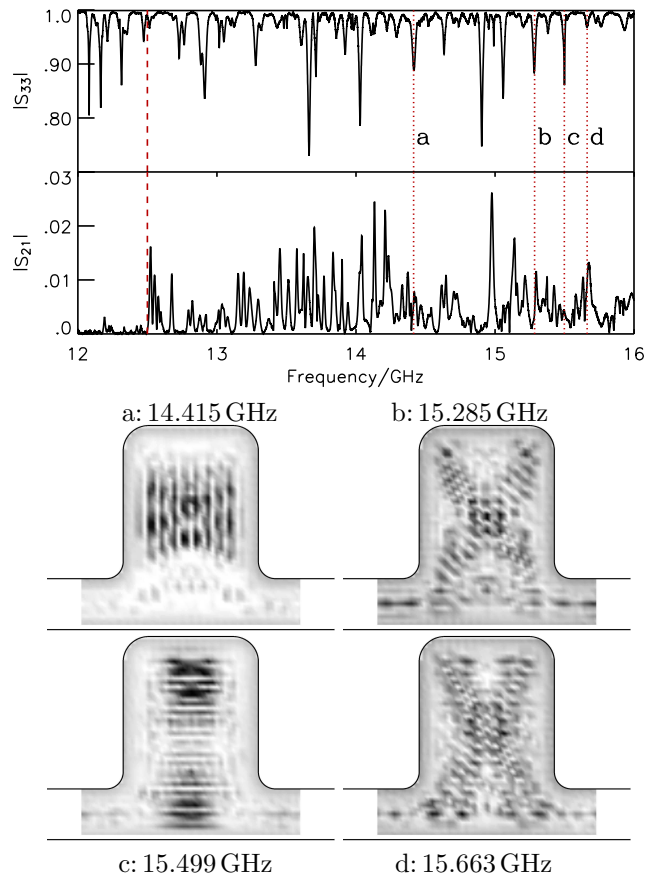


FIG. 2: Upper panel: measured reflection spectrum $|S_{33}|$ with antenna A_3 at a fixed position, and transmission spectrum $|S_{21}|$ between antennas A_1 and A_2 in the entrance and the exit port, respectively. Lower panel: wave functions for four selected frequencies obtained from the reflection at antenna A_3 as a function of the position.

the lower panel. The reflection is dominated by three scar families, two of them associated with the vertical and the horizontal bouncing ball, the third one corresponds to a cross-like structure. The cross-like structure was not observed in our previous experiments on a microwave dot with hard walls. Instead we found a scar with the shape of a loop connecting the entrance and exit ports [16].

A comparison of the reflection and the transmission measurements shows that bouncing-ball states dominating the reflection contribute only weakly to the transmission. The cross-like structures, on the other hand, exhibit maxima not only in the reflection but also in the transmission spectrum. This is in qualitative agreement with our measurements of a hard-wall microwave dot where we also found that only those states connecting the entrance and exit ports showed up to be relevant for the transport.

In the first panel of Fig. 3 the eigenfrequencies of all identified vertical bouncing ball states are shown by stars, together with two representative members of the family. Again the vertical line denotes the threshold where the

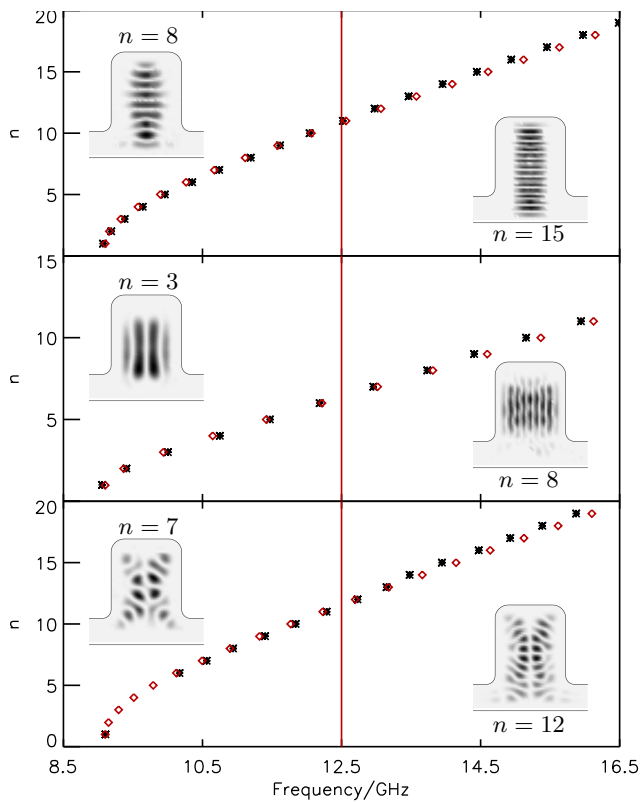


FIG. 3: Frequencies of the eigenvalues associated with the three scar families, together with two representative members of the family. Measured values are plotted by stars, calculated ones by diamonds.

attached channels open. The second and the third panels show the respective results for the horizontal bouncing ball and the cross-like scar family.

The eigenfrequencies of the members of the three families can be obtained semiclassically by means of a WKB approximation. In one-dimensional systems with two classical turning points q_1 , q_2 the action is quantized according to

$$\begin{aligned}
 S_n &= 2 \int_{q_1}^{q_2} p dq = 2 \int_{q_1}^{q_2} \sqrt{2m(E_n - V(q))} dq \\
 &= 2\pi\hbar \left(n + \frac{1}{2} \right)
 \end{aligned} \quad (3)$$

This gives an implicit expression for the eigenenergy E_n of the n -th state. Equation (3) may be applied directly to the scarred structures observed in the experiment. For the two bouncing-ball families a one-dimensional treatment is obviously justified, and the cross-like structure may be looked upon as a superposition of two one-dimensional structures, oriented along the diagonals of the billiard. For the cross-like structures, the application of the WKB approximation is somewhat questionable above 12.5 GHz where the states start to extend into the wave guides, but this leads only to small deviations.

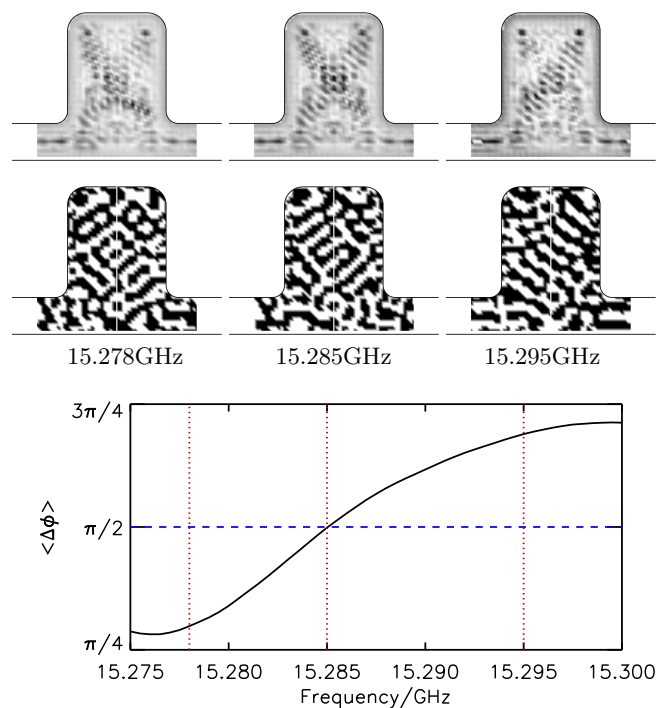


FIG. 4: Upper panel: wave functions in the low frequency wing, the center, and the high frequency wing of the resonance, marked by the letter b in Fig. 2, as obtained from a $|S_{33}|$ measurement. Middle panel: map of the corresponding phases ϕ , obtained from a S_{31} measurement, in a black-white plot. Bottom part: phase asymmetry $\langle \Delta\phi \rangle$ as a function of frequency.

Inserting the potential of Fig. 1 into Eq. (3), the eigenenergies for all members of the three families can be calculated. The eigenfrequencies are given by $\nu_n = \sqrt{2mE_n}c/(2\pi\hbar)$ and are plotted in Fig. 3 by diamonds. The overall agreement of the experimental results with the predicted theoretical values is very good. To take possible misalignments between the top and bottom plates into account, a gradient of d_{min} with an adjustable slope was allowed to improve the agreement (which was good already without this procedure). The resulting variations of d_{min} were below the experimental uncertainties given above.

The cross-like structures deserve a separate treatment. Semiclassically, the cross-like state is just an independent superposition of two structures oriented along the diagonals of the dot. Each of these structures corresponds classically to a particle that is injected from one port, then follows the diagonal trajectory, undergoing reflection at the upper corner, before leaving the billiard through the same port. Classically there is no contribution to transport. Fig. 2, on the other hand, clearly shows that the cross-like structures do contribute to the transport.

So there must be a quantum-mechanical admixture of the states, or, expressed in other words, a dynamical tunneling coupling of these states. This, however, implies that the originally two-fold degenerate states split

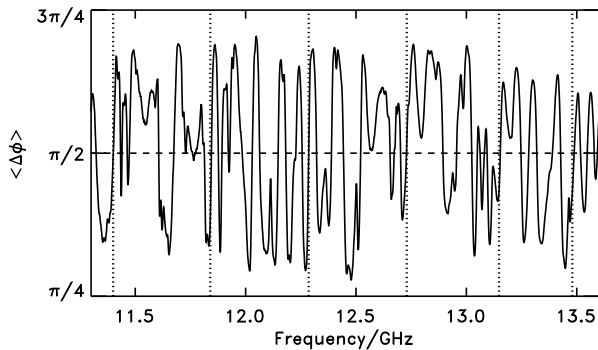


FIG. 5: Phase asymmetry $\langle \Delta\phi \rangle$ as a function of frequency. The frequencies corresponding to cross-like wave functions are marked by vertical dashed lines.

into doublets, with a symmetric wave function associated with the lower, and an anti-symmetric one with the higher energy. An inspection of the spectrum unfortunately does not show any indication of a doublet splitting (see, e.g. the resonances marked by the letters b, d in Fig. 2). This could not be expected, anyway. In the only previous microwave experiment on chaos-assisted tunneling, the observed splittings were below 1 MHz [6], much smaller than the line widths observed in the present setup. Superconducting resonators were essential to resolve such splittings. In the open microwave dot used in this work, superconducting cavities would not have been of use anyway, since the line widths are limited mainly by the openings, and not by the absorption in the walls.

Fortunately there is an alternative means to obtain direct evidence of dynamical tunneling, even in cases where the line splitting cannot be resolved. This is illustrated in Fig. 4. The upper panel shows again the wave function at 15.285 GHz, marked by the letter b in Fig. 2, but in addition the wave functions in the lower and higher frequency wing of the resonance are shown as well. There is no noticeable difference between the three patterns. A completely different impression emerges, however, when, in addition, the phases obtained from the transmission S_{31} are also considered. In the middle panel of Fig. 4 the corresponding phase maps are depicted, demonstrat-

ing without any doubt that the wave function is symmetric in the low, and anti-symmetric in the high frequency wing of the resonance. To make this even more evident, we calculated the phase asymmetry of the wave function via

$$\langle \Delta\phi \rangle = \langle \phi(x, y) - \phi(-x, y) \rangle, \quad (4)$$

where the average is over the area of the dot. $\langle \Delta\phi \rangle$ should be 0 for the symmetric case and π for the antisymmetric case. The bottom part of Fig. 4 shows the phase asymmetry for the 15.285 GHz resonance as a function of frequency. Though the ideal values 0 and π are not obtained, a change from symmetric to anti-symmetric behavior while passing through the resonance is unmistakable. Fig. 5 shows the phase asymmetry over a larger frequency range. Frequencies associated with cross-like resonances are marked by vertical dotted lines. For each of these frequencies the phase asymmetry passes through $\pi/2$, from below to above with increasing frequency. We have thus obtained a direct evidence of dynamical tunneling, using nothing but the change of the symmetry properties of the wave function upon passing through the resonances.

In conclusion, we have demonstrated a novel manifestation of dynamical tunneling in a soft-walled microwave resonator. The wave function of this system exhibits scarring due to a number of different bouncing orbits, and the eigenfrequencies of these scars were shown to be well described by the WKB approximation. In contrast to previous work, where dynamical tunneling has been identified by detecting its associated splitting of the eigenspectrum, in this report we obtained direct evidence for the tunneling process by studying the evolution of the wave function phase as a function of energy (i.e. frequency). This allowed us to identify the conditions for dynamical tunneling, even though its related level splittings were irresolvable in this system.

This work was supported by the Deutsche Forschungsgemeinschaft via individual grants. Work at the University at Buffalo is supported by the Department of Energy, the Office of Naval Research, and the New York State Office of Science, Technology and Academic Research (NYSTAR)

-
- [1] M. J. Davis and E. J. Heller, *J. Chem. Phys.* **75**, 246 (1981).
 - [2] S. Tomsovic and D. Ullmo, *Phys. Rev. E* **50**, 145 (1994).
 - [3] S. D. Frischat and E. Doron, *Phys. Rev. E* **57**, 1421 (1998).
 - [4] D. A. Steck, W. H. Oskay, and M. G. Raizen, *Science* **293**, 274 (2001).
 - [5] W. K. Hensinger, H. Häffner, A. Browaeys, N. R. Heckenberg, K. Helmerson, C. McKenzie, G. J. Milburn, W. D. Phillips, S. L. Rolston, H. Rubinsztein-Dunlop, et al., *Nature* **412**, 52 (2001).
 - [6] C. Dembowski, H.-D. Gräf, A. Heine, R. Hofferbert, H. Rehfeld, and A. Richter, *Phys. Rev. Lett.* **84**, 867 (2000).
 - [7] A. Moura, Y.-C. Lai, R. Akis, J. P. Bird, and D. K. Ferry, *Phys. Rev. Lett.* **88**, 236804 (2002).
 - [8] A. Ramamoorthy, R. Akis, J. P. Bird, R. Maemoto, D. K. Ferry, and M. Inoue, *Phys. Rev. E* **68**, 026221 (2003).
 - [9] D. K. Ferry, R. Akis, and J. P. Bird, *Phys. Rev. Lett.* **93**, 026803 (2004).
 - [10] H.-J. Stöckmann, *Quantum Chaos - An Introduction* (University Press, Cambridge, 1999).

- [11] Y.-H. Kim, M. Barth, H.-J. Stöckmann, and J. P. Bird, Phys. Rev. B **65**, 165317 (2002).
- [12] H.-M. Lauber, Ph.D. thesis, Ruprecht-Karls-Universität Heidelberg (1994).
- [13] J. P. Bird, D. M. Olatona, R. Newbury, R. P. Taylor, K. Ishibashi, M. Stopa, Y. Aoyagi, T. Sugano, and Y. Ochiai, Phys. Rev. B **52**, R14336 (1995).
- [14] R. Ketzmerick, Phys. Rev. B **54**, 10841 (1996).
- [15] E. J. Heller, J. Phys. C **99**, 2625 (1995).
- [16] Y.-H. Kim, M. Barth, U. Kuhl, and H.-J. Stöckmann, in *Let's face chaos through nonlinear dynamics*, edited by M. Robnik, Y. Aizawa, and Y. Kuramoto (Prog. Theor. Phys., Kyoto, 2003), Prog. Theor. Phys. Suppl., p. 105.